



# 1 **Lightning occurrences and intensity over the Indian region:** 2 **Long-term trends and future projections**

3 Rohit Chakraborty<sup>1</sup>, Arindam Chakraborty<sup>1,2</sup>, Ghose Basha<sup>3</sup> and Madineni Venkat Ratnam<sup>3</sup>

4 <sup>1</sup> Divecha Centre for Climate Change, Indian Institute of Science, India

5 <sup>2</sup> Centre for Atmospheric and Oceanic Studies, Indian Institute of Science, India

6 <sup>3</sup> National Atmospheric Research Laboratory, India

7 *Correspondence to:* Rohit Chakraborty ([rohitchakrab@iisc.ac.in](mailto:rohitchakrab@iisc.ac.in))

8

## 9 **Abstract**

10 Lightning activities constitute the major destructive component of thunderstorms over India. Hence,  
11 understanding the long-term variabilities of lightning occurrence and intensity and their inter-relation with various  
12 causative factors is required. Long-term (1998-2014) Tropical Rainfall Measuring Mission (TRMM) satellite-  
13 based lightning observations depict the most abundant lightning occurrences along the Himalayan foothills, the  
14 Indo-Gangetic plains and coastal regions, while the intensity of these lightning strikes are found to be strongest  
15 along the coastal regions and Bay of Bengal. In addition, both the lightning properties show a very strong  
16 intensification (~1-2.5% annually) across all Indian regions during 1998-2014 with the maximum trends along  
17 the coasts. Accordingly, a detailed statistical dominance analysis is performed which reveals total column water  
18 vapor (TCWV) to be the dominant factor behind the intensification in lightning events, while instability, measured  
19 by the convective available potential energy (CAPE), and aerosols optical depth (AOD) jointly control the  
20 lightning frequency trends. An increase in surface temperatures has led to enhanced instability hence stronger  
21 moisture transport to the upper troposphere lower stratosphere regions especially in the along the coasts. This  
22 transported moisture helps deplete the ozone concentration leading to reduced temperatures and elevated  
23 equilibrium levels which finally results in stronger and more abundant lightning events as also evidenced from  
24 the trend analysis. Consequently, the relationship between lightning and its causative factors have been expressed  
25 in form of multi-linear regression equations which are then employed on multiple global circulation models  
26 (GCM) to understand the long-term impact of urbanization on lightning over a period of 1950-2100. The analysis  
27 reveals a uniform increase in lightning occurrences, and intensity from both urbanization scenarios; however, an  
28 accelerated growth is observed in the RCP8.5 projections after the year 2050 as also observed from the surface  
29 warming trends. As a result, lightning frequency and intensity values across the Indian region are expected to  
30 increase alarmingly by ~10-25% and 15-50%, respectively, by the end of this century with highest risks along the  
31 coasts and hence it requires immediate attention from policy makers.

32 *Keywords:* Lightning; occurrences; intensity; CAPE; TCWV; AOD; GCM.

33

## 34 **1. Introduction**

35 Intense thunderstorm events form a very common climatic feature over the Indian subcontinent. These phenomena  
36 are generally accompanied by widespread lightning, wind gusts and heavy rainfall which induce various  
37 socioeconomic hazards. However, among all these by products, lightning occurrences have been found to cause



38 the greatest damage to life with a death toll of more than 2500 every year since the last two decades (Livemint,  
39 2000). In addition, the recent years have witnessed some most severe lightning calamities as per available records  
40 claiming more than 100 lives on 25 June 2020 (Washington Post, 2020).

41 Over the tropics, the non-inductive (collision based) charging interaction between ice crystals and graupel  
42 particles is found to be the major factor behind the evolution of lightning events during typical thunderstorms  
43 (Takahashi, 1978; Mansell and Ziegler, 2013). According, in this mechanism, the magnitude of charge generated  
44 per collision depends on the relative velocity of the colliding particles, the hydrometeor concentration of graupel  
45 and ice and their corresponding size distributions (Shi et al., 2015) and these in-turn are controlled by the  
46 atmospheric moisture content (total column water vapour), thermodynamic instability (convective available  
47 potential energy) and the possibility of cloud nucleation from aerosols. Additionally, Kumar and Kamra (2012)  
48 suggested that orographic lifting also has good influence on lightning but only in limited high-altitude regions of  
49 Indian Subcontinent.

50 Lightning flashes are found to be significantly correlated with convective rain, total column water vapour  
51 (TCWV), or surface relative humidity over both land and sea regions, according to previous studies (Price and  
52 Federmesser, 2006; Siingh et al., 2011; Shi et al, 2018). This is because, higher humidity levels lead to stronger  
53 hydrometeor concentration and updraft velocities, both of which contribute to intense lightning. Next, high values  
54 of instability represented by convective available potential energy (CAPE) are essential for lifting the available  
55 moisture with strong updrafts above the freezing level where they form ice and graupel particles which collide to  
56 initiate charge separation and lightning and this has already been demonstrated both theoretically and statistically  
57 in various previous research attempts (Galanki et al. 2015, Saha et al., 2017; Dewan et al. 2018).

58 Finally, coming to the impact of aerosols (AOD), a study by Shi et al., (2020) reported that the lightning  
59 flash rates are strongly correlated when  $AOD < 1$  due to the cloud/ice condensation nuclei formation characteristics  
60 from sulphates (Jin et al., 2018), desert dust (Boose et al., 2019) or even sea salt aerosols (de Leeuw et al., 2011).  
61 On the other hand, when  $AOD > 1$  then normally, larger concentrations of cloud condensation nuclei result in more  
62 supercooled droplets leading to stronger lightning (Williams and Stanfill, 2002). However, excessively high  
63 aerosol concentrations may also result in reduced cloud droplet size (Twomey et al., 1984) which reduces the  
64 efficiency of non-inductive charging process. In addition, an excess of absorptive aerosols (such as black carbon)  
65 warms the atmosphere and cools the surface (Kar et al., 2009; Talukdar et al., 2019) which further reduces the  
66 CAPE and lightning. Hence the reported relationships between lightning and aerosols is still unclear so, further  
67 studies are required to unravel it (van den Heever and Cotton, 2007).

68 Now from climatic point of view, a series of studies in recent years have shown that thunderstorm severity,  
69 lightning and its various controlling factors have been increasing prominently in the recent decades and this has  
70 been attributed to greenhouse emission induced surface warming effects both over India as well as across the  
71 globe. A study by Shindell et al. (2006) depicted that a minimum 10% increase in lightning activity can be  
72 expected due to every  $1^{\circ}\text{C}$  increase by global warming. Kandalgaonkar et al. (2005) suggested that a rise of  $1^{\circ}\text{C}$   
73 in surface temperature over India has led to a 20–40% enhancement in average lightning flash density. According  
74 to Riemann-Campe et al. (2009) and Prein et al. (2017) a recent increase of temperature has led to a rise in moisture  
75 ingress, consequently the frequency and severity of intense convective activities have shown a steep rise globally.

76 Over India, Murugavel et al. (2012) and Chakraborty et al. (2019) showed a systematic increase in CAPE  
77 which was attributed to thermodynamic instability conditions and large-scale dynamics coupled with a decrease



78 in upper tropospheric temperatures during that period. Also, satellite measurements have shown a prominent  
79 increase in aerosol concentrations over Asia due to the intense growth in urbanization and industrialization  
80 (Massie et al., 2004). Consequently, a new set of research attempts have tried to express lightning and  
81 thunderstorm severities in form of their causative factors which are employed on global climate models (GCMs)  
82 to provide future projections of extreme events (Diffenbaugh et al., 2013). Roms et al (2014) expressed the  
83 lightning flash rate in terms of the product between CAPE and precipitation rate which when implemented on 8  
84 climate models revealed an increase in lightning by  $12\pm 5\%$  per degree Celsius of warming over the USA. Later,  
85 a range of other proxies were also used over GCMs for lightning projections, but all of them also provided a  
86 similar increase in lightning both globally as well as over the USA (Bannerjee et al., 2014; Roms, 2019).  
87 However, as already hinted by Michalon et al., (1999), many years ago, most of the modelling attempts are  
88 expected to fail in providing a holistic understanding about the changing lightning climatology; and interestingly  
89 this is also found true at present as evidenced from major disagreements in magnitude of the projected trends  
90 among all the above-mentioned studies.

91 With reference to the previous sections, it has been understood that first, a very few studies on lightning has  
92 been done on the tropics and especially over the Indian region (Pereira et al., 2010) and none of the remaining  
93 attempts have tried to depict the future projections of lightning. Second, all the above-mentioned studies have  
94 utilized very poor resolution lightning datasets and hence did not provide a holistic mechanism behind the  
95 climatological variations in lightning evolution. Finally, none of these attempts have tried to see the variation of  
96 lightning radiance or intensity which is expected to be much more connected with the underlying physical  
97 processes compared to the frequency values. Thus, in the present study, high resolution lightning datasets of  
98 frequency and intensity are used over the Indian region and an attempt is made to identify the most dominant  
99 factors affecting the spatial-temporal variabilities of the lightning properties in a complete manner. Finally, the  
100 results of this dominance analysis are expressed in the form of a multi-variate regression analysis and subsequently  
101 applied on multi-model GCM datasets to generate reliable future projections of lightning occurrences and intensity  
102 over Indian for next few decades subject to various urbanization scenarios.

103 The main organization of the paper is explained as follows. A detailed illustration of the various datasets  
104 used in this study are elaborated in the datasets section. Next comes the results section which is again divided into  
105 four subsections. The first two subsections discuss the spatial distribution of lightning and its 17-year trends and  
106 they also try to identify the dominant factors responsible for the multi-decadal changes in lightning. In the next  
107 part, a probable physical mechanism is proposed to relate how the recently accelerated global warming trends can  
108 modulate the climatic intensification and abundance of lightning. However, the final subsection tries to implement  
109 the above-mentioned hypothesis on multiple long-term global climate model datasets to provide reliable future  
110 projections of lightning intensity and occurrence subject to various degrees of urbanization. In the final section of  
111 the manuscript, all the results have been summarized to produce a simplified picture which tries to quantify the  
112 long-term impacts of global warming on lightning extremes over the Indian region for future policy makers.

113

## 114 2. Datasets used

115 Lightning observations for the present study are obtained from Lightning Imaging Sensors (LISs) onboard the  
116 Tropical Rainfall Measuring Mission (TRMM) satellite which orbits the earth at 350 km elevation between  $35^\circ$   
117 N and  $35^\circ$ S at a rate of 16 orbits/day (Christian et al., 2003). These LISs can detect both intra-cloud and cloud-to-



118 ground discharges irrespective of day or night conditions with a flash detection efficiency of  $73 \pm 11$  % and  $93 \pm$   
119 4%, respectively (Boccippio et al., 2002). The lightning observations are done by monitoring illumination pulses  
120 along the 777.4 nm atomic oxygen multiplet with a very fine spatial (5.5 km) and temporal (2 ms) resolution.  
121 Every time an illumination pulse registers intensity greater than the predefined background noise level, it is  
122 considered as a separate lightning event after which all such events occurring within an integration time of 330  
123 ms are collectively considered as a single lightning flash. The view times of these flashes are also recorded  
124 separately for obtaining the monthly flash rate climatological datasets. Here it may be noted that most of the past  
125 researches have used pre-processed monthly averaged lightning flash rates after  $2.5^\circ$  and 99-day smoothing of the  
126 actual data which may have compromised the actual distribution of lightning properties in those cases. Hence, in  
127 this study, the actual lightning observations from ~95800 satellite passes have been utilized during the total  
128 availability period of 1998-2014. These lightning flash (/km<sup>2</sup>) datasets are compiled monthly and then averaged  
129 annually while the lightning radiance values (J/m<sup>2</sup>/steradian/s<sup>-1</sup>) are averaged directly on a yearly basis so that the  
130 magnitudes of both these parameters remain along the same scale of 0-1 for simplicity in analysis. However, for  
131 ease of region-wise analysis, the yearly time series of both these parameters has been analysed on a fixed grid  
132 resolution of 1 degree.

133 Next, the gridded datasets of the causative meteorological factors namely CAPE and TCWV are utilized  
134 from the Climate Forecast System Reanalysis (CFSR) developed by NOAA's National Centre for Environmental  
135 Prediction (NCEP) (<http://nomadl.ncep.noaa.gov/ncep-data/index.html>) datasets (Kalnay et al., 1996) as provided  
136 by the ESRL PSD during the period 1948-2014. These datasets are provided at a coarse spatial resolution of  $2.0^\circ$   
137  $\times 2.0^\circ$  for CAPE and  $2.5^\circ \times 2.5^\circ$  for TCWV, hence it had to be interpolated to  $1^\circ$  resolution and averaged yearly  
138 for subsequent analysis. Secondly, the datasets of aerosol content (AOD) over the maximum availability period  
139 of 2000-2014 are obtained from Level-3 (L3) MODIS TERRA Atmosphere Monthly Global Product MOD08\_M3  
140 at  $1 \times 1$  grid resolution (Platnick et al., 2015) over the Indian sub-continent. Further details can be obtained  
141 herewith ([http://gdata1.sci.gsfc.nasa.gov/daac-bin/G3/gui.cgi?instance\\_id=aerosol\\_monthly](http://gdata1.sci.gsfc.nasa.gov/daac-bin/G3/gui.cgi?instance_id=aerosol_monthly)). Gridded altitude  
142 datasets at  $0.25^\circ$  resolution are taken from GMTED2010 global digital elevation model under TEMIS project  
143 (Danielsen and Gesch, 2011). Finally, the future projections of lightning properties for various urbanization  
144 scenarios are derived using gridded datasets of the temperature, humidity and ozone profiles with aerosol optical  
145 depth at 550 nm from 11 general circulation models (GCMs) in the Coupled Model Inter-comparison Project  
146 (CMIP5) archive (website: <http://cmip-pcmdi.llnl.gov/cmip5/>) during 1950-2100. Further details of these datasets  
147 have been provided in Taylor et al. (2012) and also in subsequent sections of this study.

148

### 149 3. Results and Discussion

#### 150 3.1. Spatial distribution of lightning properties

151 The climatological average of lightning frequency shown in Figure 1(a) depicts much higher values over the land  
152 regions compared to Arabian Sea (AS) and Bay of Bengal (BoB). This is due to occurrence of stronger sensible  
153 heat fluxes over the land regions resulting in stronger updrafts, and hence more lightning (Kumar and Kamra  
154 (2012). The highest magnitude is observed along the foothills of Himalayas ( $72-95^\circ\text{E}$ ) which implies the effect of  
155 orographic convection on lightning events. In these regions, the high values of lightning flashes are found  
156 associated with the occurrence of a mountain breeze front during the afternoon hours (Boeck et al., 1999). The



157 secondary spatial maximum of lightning is observed along the coastline which can be attributed to widespread  
158 moisture advection from the adjoining seas (Kumar and Kamra, 2012).

159 The BoB experiences moderately high lightning frequencies due to high seas surface temperatures (SSTs)  
160 (above a critical threshold of 28°C according to Gadgil et al. 1984) which lead to frequent cyclonic storms and  
161 lows in this region. However, AS experience lower lightning frequencies due to lower SSTs in this region (Kumar  
162 and Kamra, 2012). Next, low lightning frequencies are observed along the peninsula due to reduced moisture  
163 supply as it is geographical bounded by mountainous terrain along the coasts from both sides. In addition,  
164 moderately high lightning frequencies are observed along the Indo-Gangetic plains (IGP) which can be due to the  
165 complex interactions among the moderate moisture supply from BoB, local instability and the CCN effects from  
166 transported (Boose et al., 2019) and emitted aerosols. Finally, very low values of lightning occurrences are seen  
167 over West Central India (WCI) which can be due to dearth of moisture supply despite the contribution from  
168 transported dust aerosols here.

169 Contrary to the occurrence climatology, the lightning radiance values (Fig. 1b) are much lower over majority  
170 of land regions which is solely because of higher values of moisture content over the coastal regions leading to  
171 more graupel (ice and hail particles concentrations above the freezing layer) as shown in Murugavel et al., 2012.  
172 Yet, the maximum values of radiance are observed exactly along the coastline regions which reduce gradually as  
173 one move further into the seas. This indicates the importance of thermal land-sea contrast which results in strong  
174 moisture advection from both land and sea breezes along the land-sea boundary (Pielke, 1974) resulting in more  
175 hydrometeors hence largest radiance. However, the presence of giant CCN marine aerosols particularly in AS (de  
176 Leeuw et al., 2011) may also act as a secondary factor. Nevertheless, AS still experiences lower lightning radiance  
177 than BoB probably due to its local meteorological factors as described earlier. Next, the lightning radiance values  
178 are found distinctly lesser over PI, WCI and HIM as they receive much less moisture than the rest of India. In  
179 Addition, a secondary maximum of radiances is observed over the IGP due to moderate moisture supply and  
180 aerosols which can act as potential ICN/CCN thereby increasing the number of colliding hydrometeors for more  
181 lightning radiance.

182 So, based on these spatial distributions of lightning occurrence and intensity, a group of 7 regions are  
183 proposed for further analysis as depicted in Fig1d. The two coastlines share high lightning occurrences as well as  
184 intensity hence are referred as Coasts. Second comes PI as a landlocked region between the Coasts with moderate  
185 values of both lightning properties. Region 3 and 4 are taken for both sea regions namely BoB and AS as their  
186 response to lightning occurrences and radiances are quite different. Next, the Himalayan foothills are considered  
187 to observe the effect of orographic convection on lightning properties independently. Then, IGP is selected since  
188 it experiences quite high lightning occurrences and intensity due to complex aerosol, instability and moisture  
189 interactions. Finally, WCI a remote inland region is considered as it experiences lower lightning properties due to  
190 meagre moisture supply despite an important contribution from land heating and aerosols.

191 The climatologically averaged distributions of lightning frequency and intensity along with 4 most potential  
192 factors influencing them (TCWV, CAPE, AOD and Altitude) for different regions are shown in Fig. S1. For  
193 lightning frequency, the mean and percentiles are highest in HIM and lowest in PI and AS. However, the extreme  
194 values for the Coasts and WCI are found to be higher than HIM because of frequent cyclonic and low-pressure  
195 systems prevalent in these regions (Fig S1a). The Lowest lightning frequency is observed over AS. The radiance  
196 and CAPE follow similar variability i.e., higher values are observed over BoB and Coasts due to more moisture



197 availability and thunderstorm occurrences while the other regions experience low to moderate values (Fig. S1b).  
198 Yet a lot of extremes are observed in IGP and WCI which implies that the occurrence of surface heating lead to  
199 higher cloud base heights and more ice-phase hydrometeors; hence more lightning in these regions as also  
200 supported from previous studies (Price, 2009; Shindell et al., 2006).

201 The total moisture content (TCWV) is found to be highest along the Coasts and adjoining sea regions as  
202 from lightning occurrences and intensity. Incidentally, the remote inland locations like PI and WCI receive much  
203 reduced moisture supply which is the primary reason behind the lower lightning radiances in those regions. Next,  
204 the IGP and WCI regions show highest values of AOD due to dust transport from Thar and Sahara deserts along  
205 with large scale emission from various anthropogenic activities which have very complex impacts on convection.  
206 Likewise, the Coasts also receive moderate aerosol supply from the adjoining seas as already described before  
207 which further support lightning formation. The HIM region depicts the highest altitude variation among all the  
208 regions, of which a significant fraction is present above 4 km height thereby supporting widespread orographic  
209 lifting induced lightning activities. Next, PI and IGP exhibit an infinitesimally small altitude variation (<500 m)  
210 which may not be sufficient to support any orographic convection. Whereas in WCI, the altitude ranges are  
211 considerably higher which in turn provides a small but vital contribution towards lightning as also supported from  
212 various past research attempts (Barros et al., 2004).

### 213 3.2. Temporal variation of lightning properties

#### 214 3.2.1. Long-term trends in lightning frequency and intensity over the Indian region

215 The 17-year time series variations of mean annual lightning frequency and radiance are depicted for seven regions  
216 and entire India in Fig. S2 along with their respective standard error values. Robust-fit regression analysis is  
217 employed to study whether there are any statistically significant trends in the lightning frequency and radiance.  
218 At the same time, a detailed description regarding the yearly % trends of lightning properties and their controlling  
219 factors (TCWV, CAPE and AOD) are depicted along with their corresponding correlation coefficients in Fig. 2.  
220 The trends of lightning frequency are found to be the highest over the Coasts, BoB and AS (with a total increase  
221 of ~30%) with reasonably high correlation coefficient values which again can be attributed to an increase of both  
222 moisture content and instability in these regions. However, the other regions depict much weaker values of both  
223 these quantities. Here it is interesting to note that IGP depicts much weaker lightning trend which may be due to  
224 the complex aerosol interactions as explained before. But in total, India has faced ~25% increase in lightning  
225 frequency (with very high correlation values) in these 17 years which is alarming and hence will be discussed in  
226 detail later in the study.

227 The mean annual lightning radiances show gradually increasing trends (with a total increase of ~20%) in  
228 almost all regions. However, the magnitudes of % trends as well as the correlation coefficients are much lesser  
229 compared to lightning frequency which implies that average radiance may not be a suitable parameter to  
230 investigate the future variations in lightning. It is known that, TRMM observes both cloud-cloud and cloud-ground  
231 types of lightning strikes together and out of the total, only the strongest 10% of the total strikes are intense enough  
232 to reach the ground in the tropics (Uman, 1986) and cause immense damage to life and property (Holle et al.,  
233 2019). Now, since it is more important to understand the trends of these extreme cases only, hence the regional  
234 trends of 90<sup>th</sup> percentile of lightning radiances is examined (Fig.2a). The trends depict a very prominent all-India  
235 trend of ~30% with higher correlation values compared to mean lightning radiance (Fig.2b). Additionally, the



236 coastal and sea regions depict much higher trends (>40%) than the rest of India which is extremely alarming for  
237 policy makers at present. However, HIM has not shown any change in lightning radiance which may due to the  
238 marginal increase in TCWV and CAPE there.

239 Further, it is investigated whether the proposed 90<sup>th</sup> percentile of radiance also agrees well with the  
240 distribution of mean radiances over every Indian region; hence the corresponding values of both the quantities for  
241 a total span of 68 seasons in 17 years are shown in Fig. S3. The figure depicts that the south Indian regions namely:  
242 BoB, Coasts, PI and AS (with stronger maritime influence) exhibit prominent correlation values between the two  
243 groups and the average ratio between the two is ~1.2; with a minimal amount of spreading which indicates that  
244 there are no external factors affecting the average radiance distribution. But the northern inland zones depict a  
245 prominent scattering between the groups (especially in IGP) and the ratio between them is also much higher (~1.4)  
246 which indicates that some external factors such as aerosols may also exert an additional impact in intensifying the  
247 radiance values well above the average radiance distributions. But overall, a good agreement is seen between the  
248 lightning radiance groups thereby supporting the suitability of using p90 radiances only in the subsequent sections.

249 Next, the trends of TCWV (Fig. 2a) depict uniform trends (0.3% yearly or 5% in total) across all regions  
250 with descent correlation values everywhere except HIM which are caused by prominent GHG induced global  
251 warming in the recent decades as shown in previous studies. CAPE which represents the atmospheric instability  
252 is the main reason for lightning evolution, hence this parameter also depicts strong interzonal variability like  
253 lightning. The Coastal regions and seas experience much stronger increase of ~9% in 17 years implying more  
254 thunderstorm activity in the present due to prominent global warming induced land sea thermal contrast. However,  
255 the rest of the country exhibits a much weaker increase (~5%) and further, the trends in IGP and WCI are even  
256 lower due to the complex aerosol effect. Finally, AOD is found to increase most significantly throughout India  
257 compared to the other parameters, however the south Indian maritime regions experience a much lower rise of  
258 ~25% compared to deep inland regions (WCI and IGP) with ~40% increase indicating that aerosols may have  
259 more dominant role in modulating the trends of lightning properties only in the continental North Indian regions.

### 260 3.2.2. Investigation of the dominant factors affecting the lightning trends over India

261 The previous sections depict a series of spatially varying complex interactions among TCWV, CAPE and AOD  
262 which resulted in an increasing trend in both lightning properties over the Indian region. Now, to identify the most  
263 dominant factors affecting the trends of lightning, a clustering analysis is done for each Indian region. Hence the  
264 datasets of lightning are taken for 15 years span (as AOD data is absent before 2000) and then they are sorted into  
265 three clusters based on magnitude. The mean and deviation of these clusters are depicted in Fig. S4 and Fig. S5  
266 with respect to corresponding values of TCWV, CAPE and AOD. Factors having dominant influence are  
267 identified as those where the parameter mean increases sharply with the clusters with minimal mutual overlapping.

268 The analysis revealed that CAPE and AOD depict good clustering for occurrences while TCWV shows the  
269 best results for radiances over Coast and BoB. AS also behaves similarly, but in case of occurrences, AOD fairs  
270 slightly better than the others implying a dominant contribution from CCN forming marine aerosol transport in  
271 this region. PI experiences lesser moisture ingress (due to its inland location) hence it relies more on dry  
272 convections which makes CAPE the major governing element for both the lightning properties. No single factor  
273 is observed to be dominant factor for lightning frequency in HIM as it mainly relies on orographic convection  
274 processes as already explained in preceding sections. But for radiance, TCWV still remains a dominant factor  
275 (Fig. S5). Next in case of IGP, CAPE exhibits fair linear clustering in occurrence while TCWV remains



276 dependable for intensity. WCI behaves similar to PI but, here a secondary influence of AOD is also observed  
277 indicating the possible impact of transported dust (acting as ICN) which catalyses the formation of ice phase  
278 hydrometeors leading to more frequent and stronger lightning events.

279 Next, the clustering analysis is performed over the entire Indian region and is shown in Fig. 3. Based on  
280 clustering and correlation analysis for lightning frequencies, CAPE emerges as the dominant factor followed by  
281 AOD. This can be supported theoretically as the generation of lightning events only requires the availability of  
282 ice phase hydrometeors above the freezing level which is achieved mainly by the lifting mechanism due to CAPE  
283 followed by the aerosol CN effect. On the other hand, in case of p90 radiance, based on clustering and correlation  
284 coefficients TCWV emerges as the single dominant feature behind the strong rise in lightning radiances all over  
285 India. This result can also be explained theoretically as the inductive/non-inductive charging density responsible  
286 for lightning radiance is far more dependent on the local hydrometeor concentrations (arising from moisture  
287 abundance) compared to their relative vertical velocities (controlled by CAPE). Now interestingly, AOD has  
288 consistently maintained a complex secondary impact on both the lightning properties depending its tendency to  
289 either favour lightning (by creating more ICN/CCN formation due to dust or sulphate aerosols) or negatively by  
290 inducing cloud burn-off effect(due to black carbon aerosols) as already discussed in preceding sections. So, a  
291 detailed study needs to be done to untangle the AOD effect in aerosol sensitive zones like IGP and WCI.

292 Now, the temporal dominance analysis is repeated quantitatively using a multi-linear regression analysis. In  
293 this step, two equations are hypothesized where lightning frequency and radiance are expressed separately as a  
294 multi-linear addition of all three controlling factors. The proposed equations can be expressed as:

$$295 \text{ Lightning frequency} = a_1 * \text{TCWV} + b_1 * \text{CAPE} + c_1 * \text{AOD} \quad (1)$$

$$296 \& \text{ Lightning intensity} = a_2 * \text{TCWV} + b_2 * \text{CAPE} + c_2 * \text{AOD} \quad (2)$$

297 Here, a, b and c represent the corresponding Multiple linear regression (MLR) coefficients for the three  
298 factors and the numbers 1 and 2 stands for lightning frequency and radiance, respectively. The corresponding  
299 variation of these MLR coefficients is shown in Fig. 4. CAPE acts as most dominating factors in all the regions  
300 except over AS where AOD influence is very high. AOD is the second most controlling parameter in lightning  
301 frequency (except over BOB and HIM). For radiances, the TCWV is the dominant factor in most regions (except  
302 over PI and WCI). The reasons for this were discussed in previous section. Again, similar to AS, AOD plays the  
303 most significant role in modulating both the lightning properties over IGP due to the role of complex aerosol-  
304 cloud interactions.

305 Finally, over the Indian region, TCWV arises as the dominant parameter controlling the climatic trends of  
306 radiances; however, for occurrence it is not so simple. Though CAPE manages to be the principal factor, yet the  
307 relative contributions of AOD followed by TCWV cannot be neglected. Next, the applicability of the proposed  
308 MLR equations for long-term studies are validated by showing the ratio between regressed and observed lightning  
309 properties (Fig4 i & j). In case of occurrences, the ratio between the two is not perfect and a small overestimation  
310 of ~5% is observed hence this bias has been corrected before using it in the coming sections. Whereas, the  
311 regressed values of radiance match perfectly with observations. Henceforth, these MLR equations have been  
312 utilized for deriving the reliable long-term projections of lightning properties in subsequent sections.

### 313 3.3 Physical mechanisms driving the increasing trends in lightning properties

314 In this section, the physical processes responsible for the increase in lightning occurrences and intensity over the  
315 Indian region will be discussed. Recent studies showed a prominent increase in aerosols and GHG emissions over





316 the Coasts, IGP and WCI as seen from the very strong increase in AOD in the recent years. This phenomenon  
317 resulted in widespread surface and atmospheric warming (Basha et al. 2017) and consequently a stronger surface  
318 evaporation and moisture production. In addition, many recent research attempts have reported a net increase in  
319 the Hadley cell and Brewer–Dobson circulation strength (Liu et al., 2012; Fu et al., 2015), which also assists in  
320 additional moisture supply. Consequently, the increased moisture in the atmosphere further accelerated the  
321 warming effect and TCWV growth in forms of a positive feedback (IPCC, 2007) primarily in the Coastal and  
322 neighbouring sea regions like BoB and AS. However, the increased moisture supply in IGP or PI is mainly due to  
323 the enhanced land-sea thermal contrast effect (due to GHG and aerosol emissions) which intensifies the moisture  
324 converges in these regions.

325 To explain how thermodynamic instability or CAPE has been increasing recently, a previous study by  
326 Chakraborty et al. (2019) is referred where long-term multi-station radiosonde observations depicted strong  
327 increasing trends in CAPE and TCWV all over Indian region with the maximum values along the coasts and  
328 surrounding inland regions. However out of the total column, the percentage trends in both instability and  
329 moisture integrals (CAPE or TCWV) are found to be particularly higher above 300 hPa pressure levels which can  
330 be associated with a gradually ascending level of neutral buoyancy (LNB/EL) during this period. Now as the EL  
331 comes very close to the 100 hPa level during intense convective events, hence an observed cooling at its immediate  
332 surroundings (135-95 hPa) is thought to be the main factor responsible for the EL ascent and CAPE increase in  
333 these regions. The main reason for considering this hypothesis is based on a study by Dhaka et al. (2010) where  
334 a very prominent anticorrelation was observed between the yearly average values of CAPE and their  
335 corresponding upper-tropospheric temperatures at 100 hPa.

336 It has been well documented in past studies that ozone molecules act as the primary heat source component  
337 at 100 hPa level (corresponding to the UTLS region) by absorbing the ultraviolet radiations (Mohankumar, 2008).  
338 Now, the multi-station radiosonde observations from Chakraborty et al. (2019) depicted a clear rise in specific  
339 humidity and a depletion in ozone mixing ratios at the same height range. These results were analogous with the  
340 findings from Forster et al. (2007) according to which the recent decades have experienced an upper tropospheric  
341 cooling due to a decrease in ozone concentration. Thus, a cooling trend at this height level can be explained by  
342 the theory that excess moisture pumped to this height by intense convections get disassociated photolytically by  
343 reactive oxygen atoms to produce two OH radicals which further decompose ozone to oxygen molecule and a  
344 reactive oxygen atom in the UTLS region (Guha et al. 2017) thereby continuing the process. Consequently, this  
345 feedback process would lead to a further ascent in EL and increase in CAPE; however, the magnitudes of the  
346 resultant CAPE intensification will be highest over the coasts and surrounding seas due to a stronger moisture  
347 advection in those regions.

348 Hence according to this hypothesis, the Coastal regions and seas experience more growth in TCWV and  
349 CAPE which lead to formation of more ice phase hydrometeors thereby promoting an accelerated rise in lightning  
350 radiance. On the other hand, larger CAPE favours more updraft velocities in the ascending particles which further  
351 increase the probability of hydrometeor collisions leading to an increased lightning frequency. However, an  
352 additional effect can also be cast by AOD by facilitating more CN formation (from dust, sulphate or sea salt  
353 aerosols) which will strengthen the above-mentioned physical mechanism thereby leading to a stronger increase  
354 in both lightning properties over the aerosol sensitive inland regions such as IGP, WCI and PI.

#### 355 **3.4 Generation of reliable future projections of lightning frequency and intensity**



#### 356 **3.4.1 Selection of GCMs for future projection analysis**

357 In this section, the MLR coefficients from previous sections are employed to provide reliable projections of future  
358 lightning activities over the Indian region. Accordingly, the datasets of CAPE, AOD and TCWV are utilized over  
359 a period of 150 years including first 55 years (1950-2005) from historical datasets and the rest (2006-2100) from  
360 two extreme future scenarios namely: RCP2.6 and 8.5. A set of 8 global climate models (GCM) of CMIP5  
361 (depicted in Table S1) are selected for analysis as all of them commonly provide the monthly mean estimates of  
362 TCWV and AOD with daily profiles of temperature, humidity and ozone. The monthly average values of CAPE  
363 are then calculated from daily T and RH profiles using the parcel approximation technique as described in past  
364 research attempts (Chakraborty et al., 2018; Narendra Reddy et al., 2018). It may be noted that, the surface-based  
365 CAPE (SB-CAPE) calculation technique has been used to obtain the current CAPE values in this study since they  
366 measure the total buoyancy experienced by the parcel raised directly from the surface to any height of the  
367 atmosphere irrespective of the prevailing atmospheric conditions, seasonality or the region where it is being  
368 derived. Now, the datasets from each of these models are interpolated to a uniform 1X1 degree resolution after  
369 which their performances are tested by comparing the simulated CAPE, TCWV and AOD values with respect to  
370 NCEP NCAR reanalysis datasets. The results of this test are represented in terms of a Taylor diagram in Fig. 5.

371 The Taylor diagram results for TCWV, CAPE and AOD unanimously reveal that models ACCESS1.3  
372 CSIRO MK3.6, MIROC5 and NOESM 1ME (represented as A, B, F and H in Fig.5.) depict good correlations  
373 over the Indian region along with lower std and rms values. In addition, the model derived monthly inputs are also  
374 validated against NCEP data for all seven regions in Fig. S6. The correlation coefficients for all regions commonly  
375 show that models ACCESS1.3 CSIRO MK3.6, MIROC5 and NOESM 1ME again show much better agreement  
376 with NCEP data. Hence these four models are considered further for lightning projection analysis. Next, the all-  
377 India averaged regressed lightning occurrences and intensity values obtained from the models during 2000-2014  
378 are plotted against their corresponding observations to check the reliability of MLR analysis on the modelled data.  
379 The results depict a fair agreement between the two sets ( $r=0.76$  in occurrences and  $0.7$  in radiance) in both the  
380 cases. However, a very prominent underestimation bias has been observed ( $\sim 24\%$  in occurrences and  $\sim 18\%$  in  
381 radiances) which is probably because the modelled datasets are of much coarser resolution than the actual  
382 observations, hence they will always depict much lesser average or variability compared to the former. However,  
383 the inter comparisons between the modelled and observed lightning properties over all the regions commonly  
384 depict quite high values of correlation with an overall underestimation bias of 17-25% thereby supporting the  
385 reliability of MLR analysis. However, the underestimation biases obtained from inter-comparison tests must be  
386 added with the regressed climatic projections for both zonal and all-India cases to get the actual lightning trends  
387 in forthcoming sections.

#### 388 **3.4.2 Examination of the 150-year trends in various factors controlling lightning**

389 The 150-year trends of various controlling factors associated with the climatic trends of lightning occurrences and  
390 intensity are shown in form of normalized % change per decade for all seven Indian regions in Fig. S7. The surface  
391 temperature trends are first considered as this parameter is closely associated with urbanization and GHG  
392 emissions and it also acts as the primary driver behind the CAPE and TCWV trends. A moderate rise in RCP2.6  
393 is observed ( $\sim 0.5\%$  per decade) which represents an all-India warming by  $\sim 1.6^\circ\text{C}$  in total while the RCP8.5  
394 scenario exhibits an extremely severe warming of  $\sim 5^\circ\text{C}$  in the Coasts, WCI, BoB and IGP which is also expected  
395 to cause a parallel increase in TCWV and CAPE in future. Next, at par with surface warming, TCWV exhibits a



396 moderate increase from RCP2.6 scenario but in case of RCP8.5, an alarming growth of ~40% is observed across  
397 India (with the largest increase in the Coasts, BoB and AS) which will definitely lead to a parallel huge change in  
398 extreme lightning radiances over the total span of 150 years.

399 In case of AOD, contrary to the extremely large increase of ~30–40% between 2000 and 2014 from MODIS,  
400 a much smaller rise of only 20% is seen during a much larger span of 150 years. Now to understand the source of  
401 this discrepancy, the 150-year time series of AOD is observed which reveals that the initially increasing trend of  
402 aerosols reverses to a strong negative trend after 2020 which results in an overall weak positive trend. The sudden  
403 decline in AOD can be explained by the fact that RCP2.6 scenarios are characterized by stringent control on GHG  
404 emissions and aerosols after 2020. However, RCP8.5 scenarios exhibit a higher overall increasing trend  
405 amounting to 60%. Now this improvement in AOD trend from the latter case is because after 2020 the AOD  
406 values saturates and then it shows a weak negative trend implying minor aerosol emission restrictions in future;  
407 hence, the net cancellation of trends does not happen here. Also, the net increase in AOD is moderate in the Coasts  
408 but much higher in aerosol sensitive regions like IGP and WCI implying even a doubling of AOD in these regions  
409 which again may cast some vital influence on the lightning frequency trends of these regions in future.

410 Next in accordance with the TCWV and temperature trends, CAPE and MLCAPE depict a 15% and 8%  
411 increase in total from RCP2.6 scenarios. Also, the CAPE trends are much higher than in MLCAPE which indicate  
412 the validity of the upper tropospheric intensification theory as explained earlier. Again, the trends in CAPE and  
413 MLCAPE are the highest being over Coasts and surrounding regions due to maximized moisture availability as  
414 also shown in the previous studies. However, the RCP8.5 scenario shows an alarmingly high total trends of ~50%  
415 and 20% in CAPE and MLCAPE respectively due to intensified global warming and moisture availability with  
416 the highest rise of ~60% over the Coasts and seas which implies the possibility of accelerated growth in lightning  
417 occurrence in these zones. However, inland regions (IGP and WCI) still show moderately high CAPE trends (due  
418 to strong surface heating and aerosol trends) which may also lead to stronger lightning frequencies there.

419 Next, the trends in EL pressure level show an expected depletion (implying an ascent in EL) from RCP2.6  
420 scenario with values between 0.5–1 % hPa per decade. However, in RCP8.5, the trends are further enhanced with  
421 a range of 1–2% per decade with the largest changes occurring in the Coasts and BoB followed by IGP and WCI  
422 due to a stronger increase in CAPE and TCWV. Similarly, the T100 cooling trends experience exactly similar  
423 behaviour as EL with ~1-degree cooling in Coastal regions from RCP2.6 scenario while in case of RCP8.5, a  
424 drastic cooling of up to ~2°C is observed in total which can highly invigorate the convective strengths leading to  
425 much stronger lightning events in future. Next, in RCP2.6 case, SHUM at 100 hPa undergoes ~0.3% increase per  
426 decade associated with a 1% decrease in ozone. Here it may be noted that the ozone depletion trends are much  
427 higher than in SHUM only because the photolytic disassociation of a single water vapour molecule with reactive  
428 oxygen atom produces two OH radicals which help in decomposition of two ozone molecules. However, using  
429 RCP8.5 scenario, these phenomena gets further amplified where -0.6% per decade increase in SHUM and (-2%)  
430 depletion in ozone is observed with highest magnitudes observed in the Coasts. Hence the results suggest that  
431 under higher surface warming (RCP8.5 scenarios), CAPE and TCWV will increase by exactly same hypothesis  
432 as shown in Section 3.3 which ultimately results in a very strong increase in lightning properties over India

433 Now, coexistent with the zonal decadal trends the all-India time series of all parameters are shown in Fig. 6.  
434 The surface temperatures depict an increase by 2 and 4 degrees, while the TCWV and CAPE also rise by 10%,  
435 50% and 20%, 40% respectively for the two pathways. However, it may be noted that the main difference in



436 TCWV trends between RCP2.6 or 8.5 scenarios mainly arises from its drastic increase in the latter case after 2050  
437 which is again attributed to the accelerated global warming conditions experienced using RCP8.5 scenarios during  
438 those decades. Next, the AOD follows a dampened increasing trend in both scenarios with the increase in latter  
439 being slightly more prominent than the former. Now these dampened AOD trends are expected to reduce the net  
440 growth in lightning occurrences (owing to AOD's prominent contribution in the lightning frequency MLR  
441 coefficients), but such effects will not be discernible in the radiance trends as it depends primarily on TCWV only.  
442 Now because of the CAPE and TCWV trends, EL has shown a prominent ascent coupled with strong UTLS  
443 cooling and increased moistening and ozone depletion trends in both urbanization scenarios. However, the trends  
444 in RCP8.5 scenario are consistently much stronger than the RCP2.6 case due to much stronger GHG induced  
445 UTLS dynamics and CAPE intensification feedback effect. In addition, the main difference between the trends  
446 from both scenarios is mostly prominent towards the end of 21<sup>st</sup> century as explained previously.

#### 447 **3.4.3 Expected overall trends in lightning frequency and intensity**

448 The 150-year trends in lightning properties for all seven Indian zones are observed in Fig. S7. The lightning  
449 occurrences depict an overall increasing trend of ~15-25% for the total 150-year span which after adjustment for  
450 underestimation bias (20-27% as in Fig. S6) provides the actual trends to be 19-31%. However, this increase of  
451 lightning occurrences is rather low compared to the 17-year trends from observations. Hence, the lightning  
452 frequency time series for each zone is investigated separately which reveal that the lightning frequencies have  
453 increased up to 2020 after which it gets saturated; nevertheless after 2050, it again started to increase up to 2100  
454 thereby leading to much lower trend values (Fig. 6). However, this type of variation can be explained by the  
455 secondary influence of AOD on lightning occurrences which also shows a dampened increase thereby  
456 compensating the impact of increasing CAPE in totality. In addition, out of all regions, the strongest increase in  
457 lightning frequency is mainly observed in the Coasts, BoB, PI, IGP and WCI which is primarily due to influence  
458 of CAPE and moisture supply in the first two and due to dry surface heating and aerosol effect in the rest. However,  
459 in RCP8.5 scenarios, a much larger trend values amounting to 29-41% are observed (after bias correction) which  
460 is mainly attributed to the stronger increase in CAPE and TCWV and a weaker decline in AOD in this case.  
461 However, the spatial distribution of the trends remains fairly like the RCP2.6 case.

462 The 150-year zonal trends in lightning radiance from RCP2.6 scenarios depict a prominent overall increasing  
463 trend of 35-54% after zone-specific bias corrections. Here the radiance trends are found to be much higher than  
464 in occurrences since the lightning radiance trends depend primarily on TCWV which also shows a prominent  
465 increase across the 150-year span. However, the net radiances are still a bit lower than the expected trends from  
466 observations due to the small declining trend contribution from aerosols. However, the RCP8.5 scenario depicts  
467 a very alarming increase amounting to (56-97% after bias correction) which can be attributed to the stronger  
468 increase in both TCWV and CAPE throughout 150 years coupled with a weaker decline in AOD. In addition, the  
469 lightning radiance trends are found to be the strongest in the Coasts and BoB, due to the accelerated rise in TCWV  
470 and CAPE while a slightly weaker trend is observed over IGP and WCI due to the compensating influence of  
471 AOD in addition to the TCWV and CAPE trends.

472 Now, at par with the zone-wise decadal lightning trends, the all- India averaged time series of lightning  
473 occurrences and intensity are depicted in Fig. 7. The lightning occurrences from RCP2.6 scenarios depict a weak  
474 increasing trend amounting to 26% (after bias correction of 24%) over the 150-year time span. As already  
475 explained, the weak trend observed is due to the cancellation between increasing trends of CAPE and TCWV



476 against a declining trend in AOD. But in case of RCP8.5, a considerable increase in lightning frequency amounting  
477 to 35% is observed which is mainly due to a strong rise in CAPE and TCWV along with a weaker decline in AOD.  
478 In case of extreme radiances, RCP2.6 scenario shows a moderate rise of ~45% throughout India (after a bias  
479 correction of 18%). However, RCP8.5 scenario depict a much higher increase by ~73% which is due to the much  
480 stronger rise in TCWV followed by CAPE with minimal contribution from AOD. In addition, an exponential rise  
481 in both TCWV and CAPE are observed after 2060 because of excessive GHG emission induced global warming  
482 thereby leading to the highest increase in lightning radiance over India after 2060.

483 Now finally, an attempt is made to estimate the net % increase in lightning properties starting from the  
484 present (2010-2020) in order to describe the probable difference in lightning trends if two extreme GHG emission  
485 policies are adopted. Under these circumstances, the lightning frequencies depict a weak rise of ~13% assuming  
486 RCP2.6 scenario but this trend would increase to ~19% in case of RCP8.5 while in the coasts, the trends may be  
487 slightly higher reaching a maximum of ~22% for the latter. Yet, these trend values are quite smaller and hence  
488 can be avoided quite easily in the future. However, in case of extreme radiance, the minimum possible increase  
489 considering stringent policy making decisions from RCP2.6 scenario is ~22% throughout India. But in absence of  
490 such restrictions (RCP8.5) the overall increase in extreme radiance will be ~37% with respect to present. In  
491 addition, due to the impact of stronger TCWV and CAPE trends, the Coastal regions can face even up to a ~50%  
492 rise in extreme lightning intensities by 2100 which poses an extreme socio-economic threat and hence requires  
493 immediate mitigation strategies from policy makers at present.

494

#### 495 **4. Summary and Conclusions**

496 Lightning activities are considered as an essential by-product of thunderstorms and they pose the greatest damage  
497 to life annually since the last few decades. However, only a few studies have been reported over India or globally  
498 which attempted to understand the evolution and distribution of lightning processes in overall and thereby provide  
499 a reliable estimate about the future projections of lightning. Hence, the present study, attempts to utilize high  
500 resolution lightning observations to explain its socio-temporal variabilities over India and also to identify the most  
501 dominant factors responsible for the evolution of such extremes. In addition, the proposed inter-relationships  
502 between lightning and its causative factors namely: moisture, instability and aerosols are also implemented in  
503 multi-model GCM datasets to derive reliable future projections of lightning properties over the Indian regions for  
504 the 21<sup>st</sup> century. The main highlights obtained from the present study include:

- 505 1. The highest climatological average of lightning occurrences is observed along the Himalayan foothills,  
506 followed by coastal regions and Indo-Gangetic plains which are mainly attributed to the influence of  
507 orographic convection, moisture ingress (due to land-sea thermal contrast) and aerosol cloud interactions.
- 508 2. Annual average values of lightning radiances are the strongest along the coastal regions and surrounding  
509 seas primarily due to the dominance of hydrometeor concentrations on the lightning charge density equations  
510 caused by enhanced moisture availability in those regions.
- 511 3. During the period 1998-2014, lightning frequencies exhibit a strong growth of ~1-2 % annually across all  
512 Indian regions with a strong inter-regional variability. However, the trend values are invariant and quite  
513 lower in the average radiance trends. Therefore, the trends in 90<sup>th</sup> percentile radiances are estimated which  
514 show prominent spatial variation with 2-2.5% increase annually along Coasts, BOB, PI and IGP. These zonal  
515 diversities in the lightning trends are also supported by the corresponding CAPE and AOD trends.



- 516 4. The clustering and multi-linear regression dominance tests depict that over India as a whole, atmospheric  
517 moisture (TCWV) is the principle factor controlling the lightning extreme radiance trends, while instability  
518 (CAPE) and aerosols (AOD) jointly play a strong role behind lightning frequency variation. However, in the  
519 latter, the proposed inter-relationships are found to deviate from region to region due to complex aerosol-  
520 cloud interactions towards thunderstorm genesis and lightning evolution.
- 521 5. Results from previous research attempts are employed to explain the underlying physical mechanism of these  
522 trends which inferred that an increase in surface temperatures has led to higher instability and moisture  
523 transport to the UTLS regions. This moistening resulted in ozone depletion and cooling which further  
524 uplifted the equilibrium levels leading to stronger CAPE and more ice-phase collisions above the freezing  
525 level; and eventually this complex feedback procedure ultimately leads to stronger and much more lightning  
526 events. A schematic of these processes has been depicted in Fig. 8.
- 527 6. The above-mentioned hypothesis is found to be most prominent in the coasts and surrounding seas due to its  
528 high moisture abundance. However, in addition to these factors, this mechanism will also be further  
529 invigorated/inhibited based on the prevailing RCP scenarios and also depending on the region-specific  
530 aerosol input on convective processes as discussed before.
- 531 7. These observed inter-relationships are expressed in form of multi-linear regression equations and then  
532 implemented on 4 suitable GCMs out of 8 available models during 1950-2100. The resulting multi-decadal  
533 projections reveal prominent trends in surface temperatures, moisture, instability and subsequent ozone and  
534 moisture concentrations in UTLS as proposed. However, a difference in urbanization rates led to much  
535 sharper trends in all parameters particularly after 2050 in the RCP8.5 case.
- 536 8. Consequently, the regressed lightning projections also depict an increase in both occurrences and intensity.  
537 However, the increasing trends are consistently higher in the RCP8.5 case. In addition, the increase in  
538 lightning frequency is found to be much slower than in case of intensities due to the dominant impact of  
539 AOD trends which also show a comparative saturation or decrease after 2020. This can be attributed to a  
540 probable increase in GHG emission restrictions by policy makers in near future.
- 541 9. Finally, the net intensification in lightning properties by 2100 with respect to present values depict that  
542 number of occurrences would increase moderately by (10-17 % and 16-23%) for RCP2.6 and 8.5 scenarios.  
543 However, extreme lightning radiances will increase much faster by 16-27% and 32-50% in RCP2.6 and 8.5,  
544 throughout India.
- 545 10. In addition to the overall trends, certain regions like the coasts and surrounding seas are prone to be at the  
546 higher lightning risk in future since they show much stronger increasing trends of ~50% (for radiance) in  
547 absence of stringent GHG emission restrictions (as in RCP8.5) which is extremely alarming and hence should  
548 be immediately addressed by policy makers.
- 549 It may be noted that this is the first ever study to use high resolution observations of lightning radiance as well as  
550 frequency over the Indian region where a holistic inter-relation between lightning and its causative factors have  
551 been proposed, tested and then implemented over a set of GCMs so as to provide a set of future projections for  
552 both lightning properties till the end of this century. Now, the lightning projections laid out in this study can be  
553 considered as reliable for forthcoming research attempts since both the equations and the models have been  
554 repeatedly validated against observational datasets. Nevertheless, the projected lightning increase due to global  
555 warming in this study is found to be much lesser than that obtained by simultaneous studies over the United States



556 (as evidenced from Roms (2019)), the reason for which can be possibly attributed either to stronger urbanizations  
557 conditions in those regions or the choice of lightning proxies and GCM datasets used in that study.

558 However, from a closer point of view, the present study still has certain shortcomings. The primary limitation  
559 is that it tries to provide an overall explanation for lightning trends over the Indian region. However, for specific  
560 regions of the country such as WCI, HIM or IGP, secondary mechanisms from orographic influence or aerosol  
561 effects (both radiative or microphysical) can also play a stronger role on the lightning trends and hence this  
562 requires another dedicated study to address these issues. Secondly, the observed trends may vary strongly when  
563 observed for separate seasons which have been averted here to provide a more focussed investigation on the  
564 climatic trends of lightning. Finally, this study provides an overall mechanism of lightning; however, this  
565 procedure may not be followed for all types of thunderstorm events, hence in future a suite of numerical models  
566 and observations are required to explain how individual lightning events may be impacted by the complex aerosol,  
567 instability and moisture interactions within the cloud over various meteorological conditions and Indian locations.

568

#### 569 **Data availability**

570 High resolution lightning datasets for the present study have been obtained from LIS archives of NASA Global  
571 Hydrology Resource Centre DAAC, U.S.A. ([https://ghrc.nsstc.nasa.gov/lightning/data/data\\_lis\\_trmm.html](https://ghrc.nsstc.nasa.gov/lightning/data/data_lis_trmm.html) last  
572 access: 16 December 2020). Gridded datasets of CAPE and TCWV are utilized from the CFSR reanalysis archives  
573 developed by NCEP (<http://nomadl.ncep.noaa.gov/ncep-data/index.html> last access: 10 December 2020). The  
574 datasets of AOD are utilized from Level-3 (L3) MODIS TERRA Atmosphere Monthly Global Product  
575 MOD08\_M3 ([http://gdata1.sci.gsfc.nasa.gov/daac-bin/G3/gui.cgi?instance\\_id=aerosol\\_monthly](http://gdata1.sci.gsfc.nasa.gov/daac-bin/G3/gui.cgi?instance_id=aerosol_monthly) last access: 10  
576 December 2020). Finally, the future projections of lightning properties are derived from 11 general circulation  
577 models (GCMs) in the Coupled Model Inter-comparison Project (CMIP5) archive (website: [http://cmip-  
578 pcmdi.llnl.gov/cmip5/](http://cmip-pcmdi.llnl.gov/cmip5/) last access: 1 December 2020).

579

#### 580 **Author contributions**

581 RC performed complete analysis and wrote the first draft. MVR and SGB provided the initial concept and did the  
582 main editing while AC contributed to supervision, discussion, and editing.

583

#### 584 **Competing interests**

585 The authors declare that they have no conflict of interest.

586

#### 587 **Acknowledgments**

588 One of the authors (Rohit Chakraborty) thanks the Institute of Eminence Grant and Department of Science and  
589 Technology for providing support under C V Raman Post-Doctoral fellowship and INSPIRE Faculty Research  
590 Grant. He also acknowledges the Indian Institute of Science, for providing necessary support for this work. AC  
591 acknowledges funding from the National Monsoon Mission, Ministry of Earth Sciences, Govt of India.

592

593

594

595



596 **References**

- 597 Banerjee, A., Archibald, A. T., Maycock, A. C., Telford, P., Abraham, N. L., Yang, X., Braesicke, P., and Pyle,  
598 J. A.: Lightning NO<sub>x</sub>, a key chemistry–climate interaction: impacts of future climate change and consequences  
599 for tropospheric oxidising capacity, *Atmos. Chem. Phys.*, 14, 9871–9881, [https://doi.org/10.5194/acp-14-9871-](https://doi.org/10.5194/acp-14-9871-2014)  
600 2014, 2014.
- 601 Barros, A. P., and T. J. Lang.: Exploring spatial modes of variability of terrain-atmosphere interactions in the  
602 Himalayas during monsoon onset, *Hydrosci. Rep. Ser. 03–001*, 51, Div. of Eng. and Appl. Sci., Harvard Univ.,  
603 Cambridge, Mass., 2003.
- 604 Basha, G., Kishore, P., Ratnam, M. V., Jayaraman, A., Kouchak, A. A., Ouarda, T. B. M. J., and Velicogna, I.:  
605 Historical and Projected Surface Temperature over India during 20th and 21<sup>st</sup> century, *Sci. Rep.*, 7, 2987, 2017
- 606 Boccippio, D. J., Koshak, W. K. and Blakeslee, R.J.: Performance assessment of optical transient detector and  
607 lightning imaging sensor, part I: diurnal variability. *J. Atmos. Ocean. Technol.* 19, 1318–1332, 2002.
- 608 Boeck, W. L., Mach, D., Goodman, S. J., and Christian Jr. H. J.: Optical observations of lightning in Northern  
609 India, Himalayan mountain countries and Tibet, in 11th International Conference on Atmospheric Electricity,  
610 NASA Conf. Publ., NASA/CP-1999-209261, 420–423, 1999.
- 611 Boose, Y., Baloh, P., Plötze, M., Ofner, J., Grothe, H., Sierau, B., Lohmann, U., and Kanji, Z. A.: Heterogeneous  
612 ice nucleation on dust particles sourced from nine deserts worldwide – Part 2: Deposition nucleation and  
613 condensation freezing, *Atmos. Chem. Phys.*, 19, 1059–1076, h
- 614 Chakraborty, R., Basha, G., and Ratnam, M. V.: Diurnal and long-term variation of instability indices over  
615 tropical region in India, *Atmos. Res.*, 207, 145–154, <https://doi.org/10.1016/j.atmosres.2018.03.012>, 2018.
- 616 Chakraborty, R., Venkat Ratnam, M., and Basha, S. G.: Long-term trends of instability and associated  
617 parameters over the Indian region obtained using a radiosonde network, *Atmos. Chem. Phys.*, 19, 3687–3705,  
618 <https://doi.org/10.5194/acp-19-3687-2019>, 2019.
- 619 Christian, H. J., Blakeslee, R. J., Boccippio, D. J., Boeck, W. J., Buechler, D. E., Driscoll, K. T., Goodman, S.  
620 J., Hall, J. M., Koshak, W. J., Mach, D. M. and Stewart, M. F.: Global frequency and distribution of lightning  
621 observed from space optical transient detector. *J. Geophys. Res.* 108, 4005. 2003.
- 622 Danielson, J. J. and Gesch, D. B.: Global multi-resolution terrain elevation data 2010 (GMTED2010): U.S.  
623 Geological Survey Open-File Report 2011-1073, pp 26, 2011.
- 624 de Leeuw, G., Andreas, E. L., Anguelova, M. D., Fairall, C. W., Lewis, E. R., O'Dowd, C., Schulz, M. and  
625 Schwartz, S. E: Production flux of sea spray aerosol. *Rev. Geophys.* 49, RG2001.  
626 <http://dx.doi.org/10.1029/2010RG000349>, 2011.
- 627 Dewan, A., Ongee, E. T., Rafiuddin, M., Rahman, M. M. and Mahmood, R.: Lightning activity associated  
628 precipitation and CAPE over Bangladesh. *Int. J. Climatol*, 38, 1649-1660. doi:[10.1002/joc.5286](https://doi.org/10.1002/joc.5286), 2018.
- 629 Dhaka, S. K., Sapra, R., Panwar, V., Goel, A., Bhatnagar, R., and Kaur, M.: Influence of large-scale variations  
630 in convective available potential energy (CAPE) and solar cycle over temperature in tropopause region at Delhi  
631 (28.3\_N, 77.1\_E), Kolkata (22.3\_N, 88.2\_E), Cochin (10\_N, 77\_E), and Trivandrum (8.5\_N, 77.0\_E) using  
632 radiosonde during 1980–2005, *Earth Planets Space*, 62, 319–331, 2010.
- 633 Diffenbaugh, N. S., Scherer, M., and Trapp, R. J.: Robust increases in severe thunderstorm environments due to  
634 greenhouse forcing, *P. Natl. Acad. Sci. USA*, 110, 16361–16366, 2013.
- 635 Forster, P. M., Bodeker, G., Schofield, R., Solomon, S., and Thompson, D.: Effects of ozone cooling in the  
636 tropical lower stratosphere and upper troposphere, *Geophys. Res. Lett.*, 34, L23813, 2007.





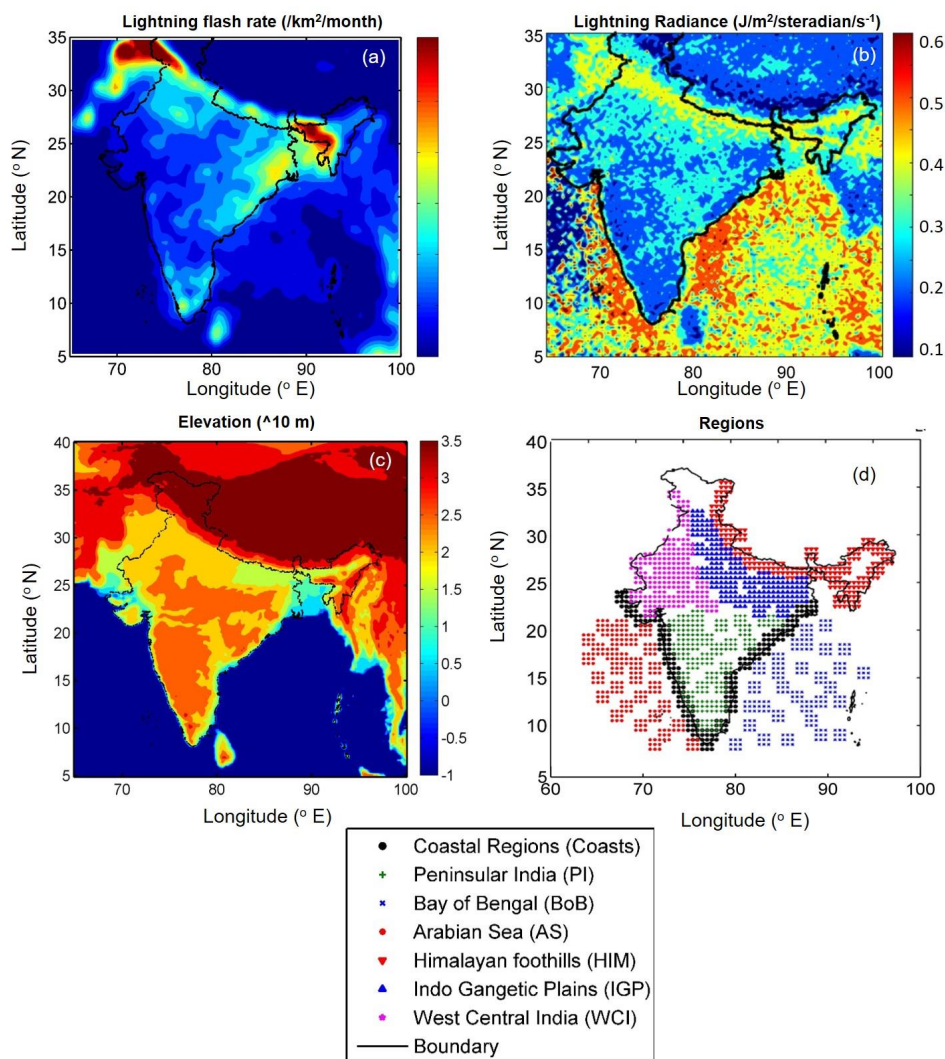
- 637 Fu, Q., Lin, P., Solomon, S., and Hartmann, D. L.: Observational evidence of strengthening of the Brewer-  
638 Dobson circulation since 1980, *J. Geophys. Res.-Atmos.*, 120, 10214–10228, 2015.
- 639 Gadgil, S., Joseph, P.V. and Joshi, P.V.: Ocean–atmosphere coupling over monsoon regions. *Nature* 312, 141–  
640 143, 1984.
- 641 Galanaki E, Kotroni V, Lagouvardos K and Argiriou A.: A ten-year analysis of cloud-to-ground lightning  
642 activity over Eastern Mediterranean region. *Atmos. Res.* 166, 213–222., 2015
- 643 Guha, B. K., Chakraborty, R., Saha, U. and Maitra, A.: Tropopause height characteristics with ozone over  
644 stratospheric moistening during intense convection over Indian sub-continent, *Global Planet. Change*, 158, 1–  
645 12, 2017.
- 646 Holle, R. L., Dewan, A., Said, R., Brooks, W.A., Hossain, M.F. and Rafiuddin, M.: Fatalities related to lightning  
647 occurrence and agriculture in Bangladesh. *Int. J. Disaster Risk Reduct.*, 41, 101264, 2019.
- 648 IPCC TAR-07, <https://www.ipcc.ch/site/assets/uploads/2018/03/TAR-07.pdf>, 2018.
- 649 Jin, Q., Grandey, B. S., Rothenberg, D., Avramov, A., and Wang, C.: Impacts on cloud radiative effects induced  
650 by coexisting aerosols from international shipping and maritime DMS emissions, *Atmos. Chem. Phys.*, 18,  
651 16793–16808, <https://doi.org/10.5194/acp-18-16793-2018>, 2018.
- 652 Kalnay, E. Kanamitsu, M. Kistler, R. Collins, W., Deaven, D. Gandin, L. Iredell, M. Saha, S. White, G. Woollen,  
653 J. Zhu, Y. Leetmaa, A. Reynolds, B. Chelliah, M. Ebisuzaki, W. Higgins, W. Janowiak, J. Mo, K. C. Ropelewski,  
654 C. Wang, J. Roy, J. and Dennis, J.: The NCEP/NCAR 40-Year Reanalysis Project. *Bull. Amer. Meteor. Soc.*,  
655 77, 437–472, 1996.
- 656 Kandalgaonkar, S. S., Tinmaker, M. I. R., Kulkarni, J. R., Nath, A. S. and Kulkarni, M. K.: Spatio-temporal  
657 variability of lightning activity over the Indian region. *J. Geophys. Res.* 110, D11108, 2005.
- 658 Kar, S. K., Liou, Y. A. and Ha, K. J.: Aerosol effects on the enhancement of cloud-to-ground lightning over  
659 major urban areas of South Korea. *Atmos. Res.* 92, 80–87, 2009.
- 660 Kumar, P. R. and Kamra, A. K.: Land–sea contrast in lightning activity over the sea and peninsular regions of  
661 South/Southeast Asia, *Atmos. Res.*, 118, 52–67, 2012.
- 662 Liu, J., Song, M., Hu, Y., and Ren, X.: Changes in strength and width of Hadley Circulation since 1871, *Clim.*  
663 *Past*, 8, 1169– 1175, 2012.
- 664 Livemint: [https://www.livemint.com/Politics/ZhfsGYczjwDo22DtvdDKfN/Lightnings-a-bigger-killer-than-](https://www.livemint.com/Politics/ZhfsGYczjwDo22DtvdDKfN/Lightnings-a-bigger-killer-than-you-think.html)  
665 [you-think.html](https://www.livemint.com/Politics/ZhfsGYczjwDo22DtvdDKfN/Lightnings-a-bigger-killer-than-you-think.html), last access: 19 September 2020
- 666 Mansell, E. R. and Ziegler, C. L.: Aerosol effects on simulated storm electrification and precipitation in moment  
667 microphysics model. *J. Atmos. Sci.* 70, 2032–2050, 2013.
- 668 Massie, S. T., Torres, O. and Smith, S. J.: Total Ozone Mapping Spectrometer (TOMS) observations of increases  
669 in Asian aerosol in winter from 1979 to 2000. *J. Geophys. Res.* 109, D18211, 2004.
- 670 Michalon, N., Nassif, A., Saouri, T., Royer, J. F. and Pontikis, C.A.: Contribution to the climatological study of  
671 lightning. *Geophys. Res. Lett.* 26, 3097–3100, 1999.
- 672 Mohanakumar, K.: *Stratosphere-troposphere interactions: introduction*, Springer Science Business Media, the  
673 Netherlands, 2008.
- 674 Murugavel, P., Pawar, S. D., and Gopalakrishnan, V.: Trends of convective available potential energy over the  
675 Indian region and its effect on rainfall, *Int. J. Climatol.*, 32, 1362–1372, 2012.



- 676 Narenda Reddy, N., Venkat Ratnam, M., Basha, G., and Ravikiran, V.: Cloud vertical structure over a tropical  
677 station obtained using long-term high-resolution radiosonde measurements, *Atmos. Chem. Phys.*, 18, 11709–  
678 11727, 2018.
- 679 Pereira, Felix B., Priyadarsini, G. and Girish, T.E.: A possible relationship between global warming and  
680 lightning activity India during period 1998–2009. arXiv: General Physics, arxiv.org/pdf/1012.3338, 2010
- 681 Pielke, R.A.: A three-dimensional numerical model of the sea breezes over south Florida. *Mon. Weather Rev.*  
682 102, 115–139, 1974.
- 683 Platnick, S., et al.: MODIS Atmosphere L3 Monthly Product. NASA MODIS Adaptive Processing System,  
684 Goddard Space Flight Center, USA, 2015.
- 685 Prein, A. F., Rasmussen, R. M., Ikeda, K., Liu, C., Clark, M. P., Holland, G. J.: Future intensification of hourly  
686 precipitation extremes, *Nat. Clim. Change*, 7, 48–52, 2017.
- 687 Price, C.: Will drier climate result in lightning?, *Atmos. Res.* 91, 479–484, 2009.
- 688 Price, C. and Federmesser, B.: Lightning-rainfall relationships in Mediterranean winter thunderstorms.  
689 *Geophys. Res. Lett.* 33, L07813. 2006.
- 690 Riemann-Campe, K., Fraedrich, K., and Lunkeit, F.: A global climatology of convective available potential  
691 energy (CAPE) and convective inhibition (CIN) in ERA-40 reanalysis, *Atmos. Res.*, 93, 534–545, 2009
- 692 Romps, D. M., Seeley, J. T., Vollaro, D and Molinari, J.: Projected increase in lightning strikes in the United  
693 States due to global warming, *Science*, 346, 6211, 2014.
- 694 Romps, D. M.: Evaluating the future of lightning in cloud-resolving models. *Geophys. Res. Lett.*, 46. 2019.
- 695 Saha, U., Siingh, D., Kamra, A. K., Galanaki, E., Maitra, A., Singh, R. P., Singh, A. K., Chakraborty, S. and  
696 Singh, R.: On the association of lightning activity and projected change in climate over the Indian sub-continent,  
697 *Atmos. Res.*, 183, 173-190, 2017.
- 698 Shi Z., Tana, Y. B., Tang H. Q, Sunc, J., Yanga, Y., Penga, L. and Guo, X.F.: Aerosol effect on land-ocean  
699 contrast in thunderstorm electrification and lightning frequency, *Atmos. Res.*, 164–165, 131–141, 2015.
- 700 Shi, Z., Tan, Y. B., Liu, Y., Liu, J., Lin, X., Wang, M. and Luan, J.: Effects of relative humidity on electrification  
701 and lightning discharges in thunderstorms. *Terr. Atmos. Ocean. Sci.*, 29, 695-708, [https://doi: 10.3319/  
702 TAO.2018.09.06.01](https://doi.org/10.3319/TAO.2018.09.06.01), 2018
- 703 Shi Z, Wang H. C., Tan, Y. B., Li, L.Y. and Li, C. S.: Influence of aerosols on lightning activities in central  
704 eastern China. *Atmos Sci Lett.*, 21, e957. 2020.
- 705 Shindell, D. T., Faluvegi, G., Unger, N., Aguilar, E., Schmidt, G. A., Koch, D. M., Bauer, S. E. and Miller, R.  
706 L.: Simulations of preindustrial, present-day, and 2100 conditions in the NASA GISS composition and climate  
707 model G-PUCCINI. *Atmos. Chem. Phys.* 6, 4427–4459, 2006.
- 708 Singh, D., Singh, R. P., Singh, A. K., Kulkarni, M. N., Gautam, A. S. and Singh, A. K.: Solar activity, lightning  
709 and climate. *Surv. Geophys.* 32, 659–703. 2011.
- 710 Takahashi, T.: Riming electrification as a charge separation mechanism in thunderstorms, *J. Atmos. Sci.*, 35,  
711 1536–1548, 1978.
- 712 Talukdar, S., Venkat Ratnam, M., Ravikiran, V. Chakraborty, R.: Influence of black carbon on atmospheric  
713 instability. *J. Geophys. Res.: Atmos.*, 124, 5539– 5554. 2019.



- 714 Taylor, K. E., Stouffer, R. J. and Meehl, G. A.: An Overview of CMIP5 and Experiment Design. Bull. Amer.  
715 Meteor. Soc., 93, 485–498, 2012.
- 716 Twomey, S. A., Piepgrass, M. and Wolfe, T. L.: An assessment of the impact of pollution on global cloud  
717 albedo. Tellus 36B, 356–366. 1984.
- 718 Uman, M.: All About Lightning Ch. 8, p. 68. Dover Publication Inc, 1986
- 719 van den Heever, S. C. and Cotton, W. R.: Urban aerosol impacts on downwind convective storms. J.  
720 Appl.Meteorol. Climatol. 46, 828–850. 2007
- 721 Washington Post: [https://www.washingtonpost.com/world/lightning-strikes-kill-more-than-100-in-](https://www.washingtonpost.com/world/lightning-strikes-kill-more-than-100-in-india/2020/06/26/4c010886-b71c-11ea-9a1d-d3db1cbe07ce_story.html)  
722 [india/2020/06/26/4c010886-b71c-11ea-9a1d-d3db1cbe07ce\\_story.html](https://www.washingtonpost.com/world/lightning-strikes-kill-more-than-100-in-india/2020/06/26/4c010886-b71c-11ea-9a1d-d3db1cbe07ce_story.html), last access: 19 September 2020
- 723 Williams, E. and Stanfill, S.: The physical origin of the land–ocean contrast in lightning activity. C. R. Phys. 3,  
724 1277–1292, 2002.
- 725



726

727 **Figure 1:** Climatological mean (a) lightning flash rate, (b) lightning radiance over India averaged during 1998-2014. (c)  
728 Altitude above mean sea level in log10 scale (Seas denoted by -) (d) Representation of seven regions used in the study

729

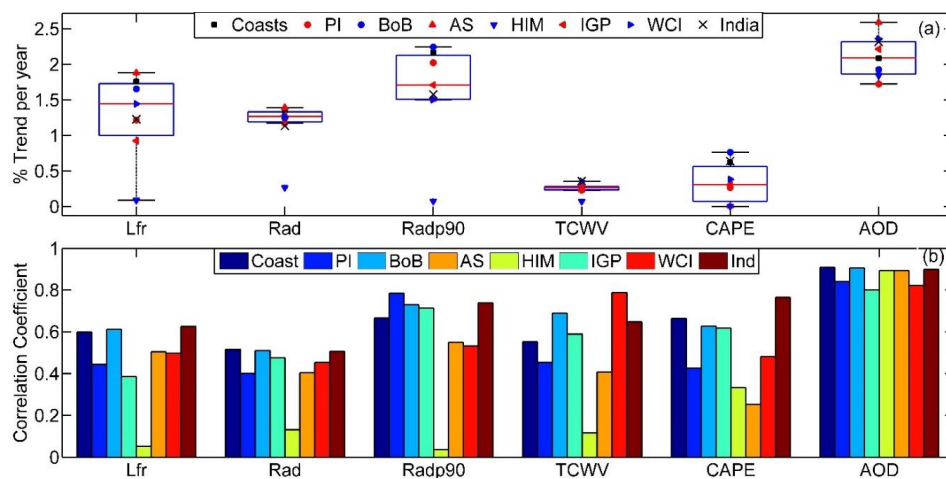
730

731

732

733

734



735

736 **Figure 2:** (a) % yearly trends in lightning flash rate (Lfr), Average radiance (Rad) and 90<sup>th</sup> percentile of radiance (Radp90)  
 737 with TCWV, CAPE and AOD over seven regions and all India datasets. (b) Correlation coefficients corresponding to this trend  
 738 values.

739

740

741

742

743

744

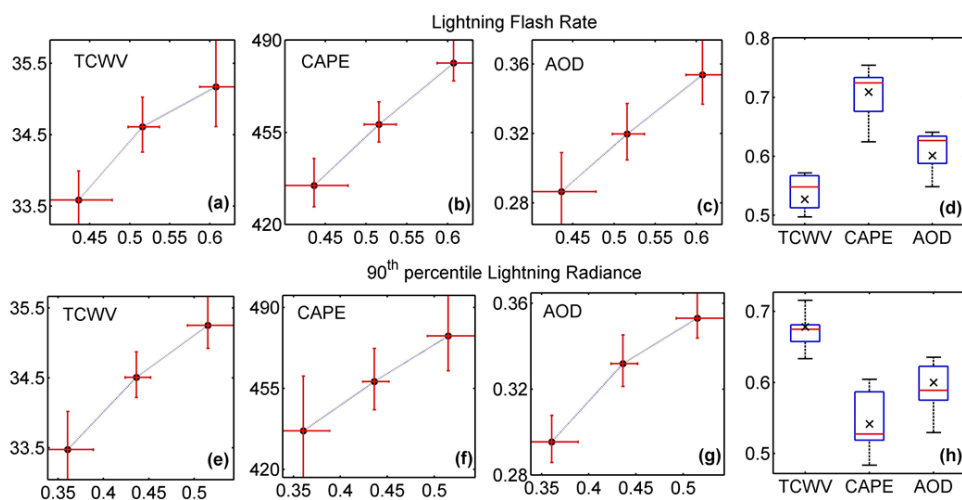
745

746

747

748

749



750

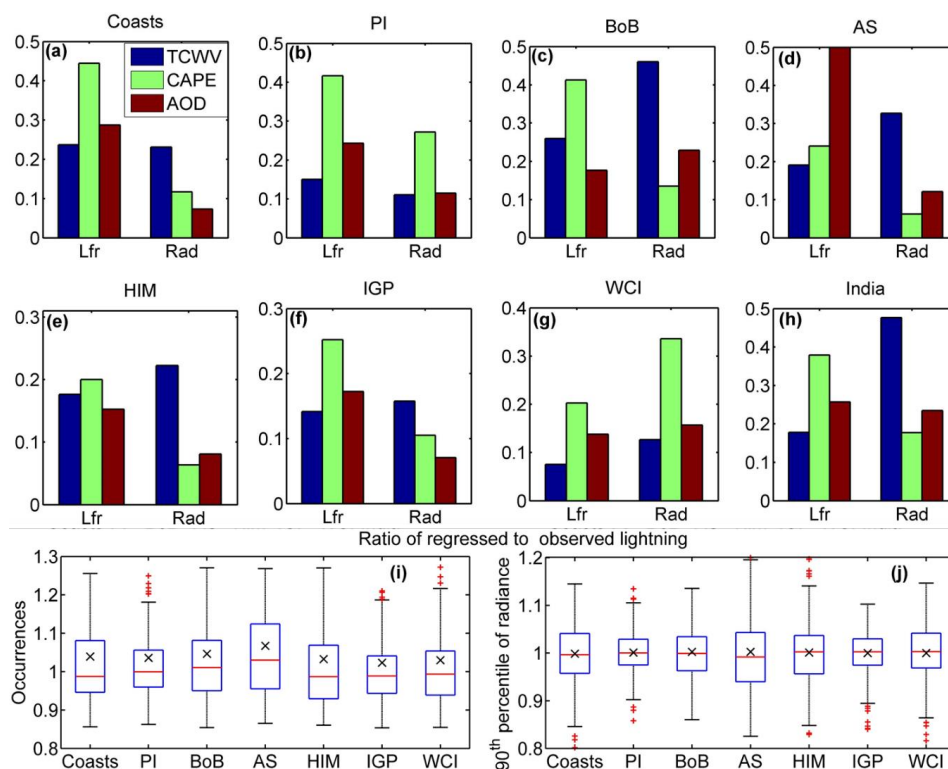
751 **Figure 3.** Temporal dominance cluster analysis results of lightning frequency and extreme radiances with respect to (a,e)  
752 TCWV, (b,f) CAPE and (c,g) AOD over entire Indian region, (d,h) distribution of correlation coefficient due to zonal clustering  
753 for both lightning parameters.

754

755

756

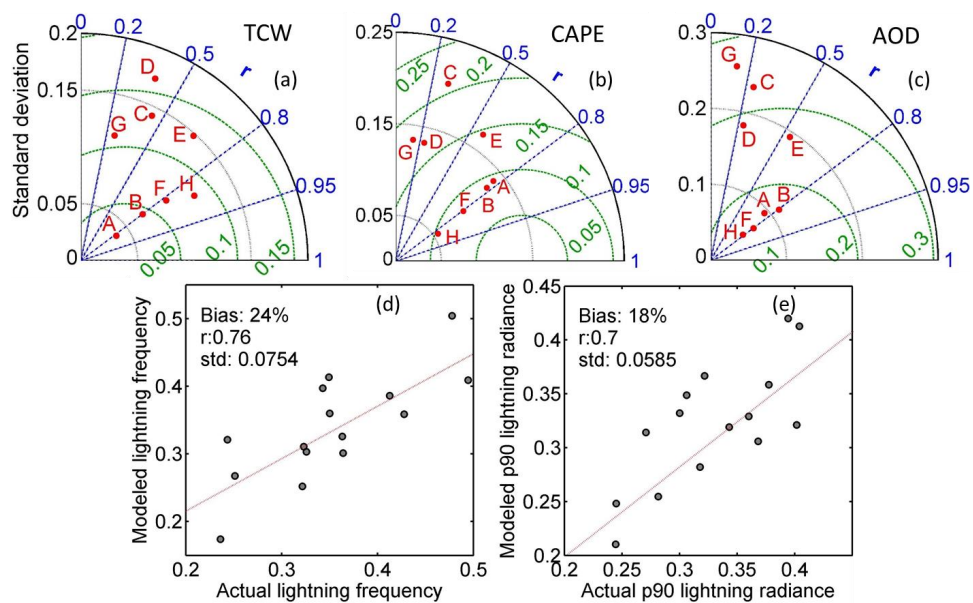
757



758

759 **Figure 4:** Temporal dominance analysis MLR coefficients of TCWV, CAPE and AOD for lightning frequency and radiance  
 760 over (a) Coasts, (b) PI, (c) BoB, (d) AS, (e) HIM, (f) IGP, (g) WCI and (h) all India, (i,j) Zonal distribution of ratios between  
 761 regressed and observed lightning frequency (Lfr) and 90<sup>th</sup> percentile of radiance (Radp90) over seven Indian regions.

762



763

764 **Figure 5:** Taylor diagram representing the performance of 8 GCMs used in the study with respect to (a) TCWV, (b) CAPE  
765 and (c) AOD, (d,e) Covariation between regressed lightning properties from model mean with respect to observations for  
766 occurrences and intensity.

767

768

769

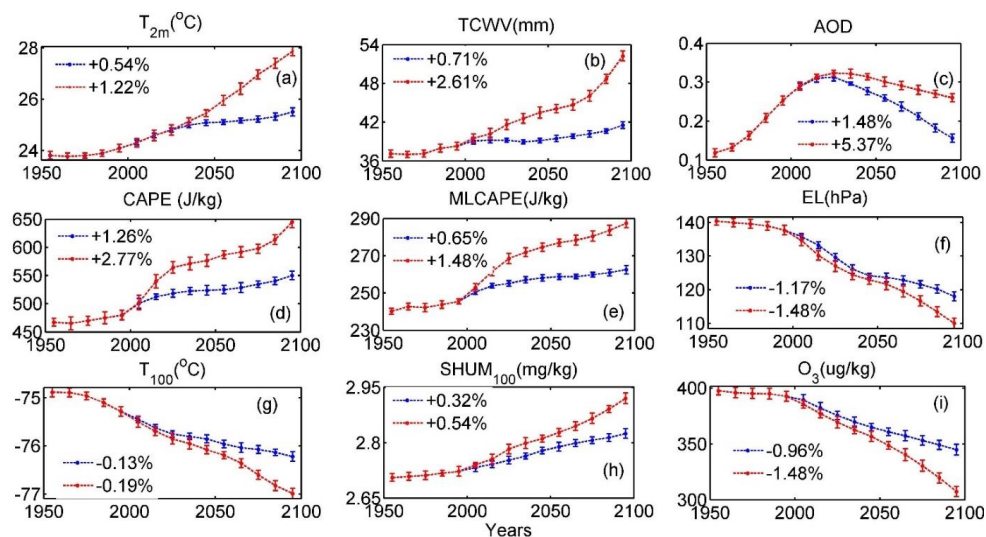
770

771

772

773





774

775 **Figure 6:** 150-year multi-model all-India average projections of various parameters using RCP 2.6 (blue) and RCP 8.5 (red)  
776 scenarios for (a) 2 metre temperature, (b) TCWV, (c) AOD, (d) CAPE, (e) MLCAPE, (f) EL, (g) Temperature 100 hPa, (h)  
777 Specific humidity, (i) Ozone mixing ratio same level.

778

779

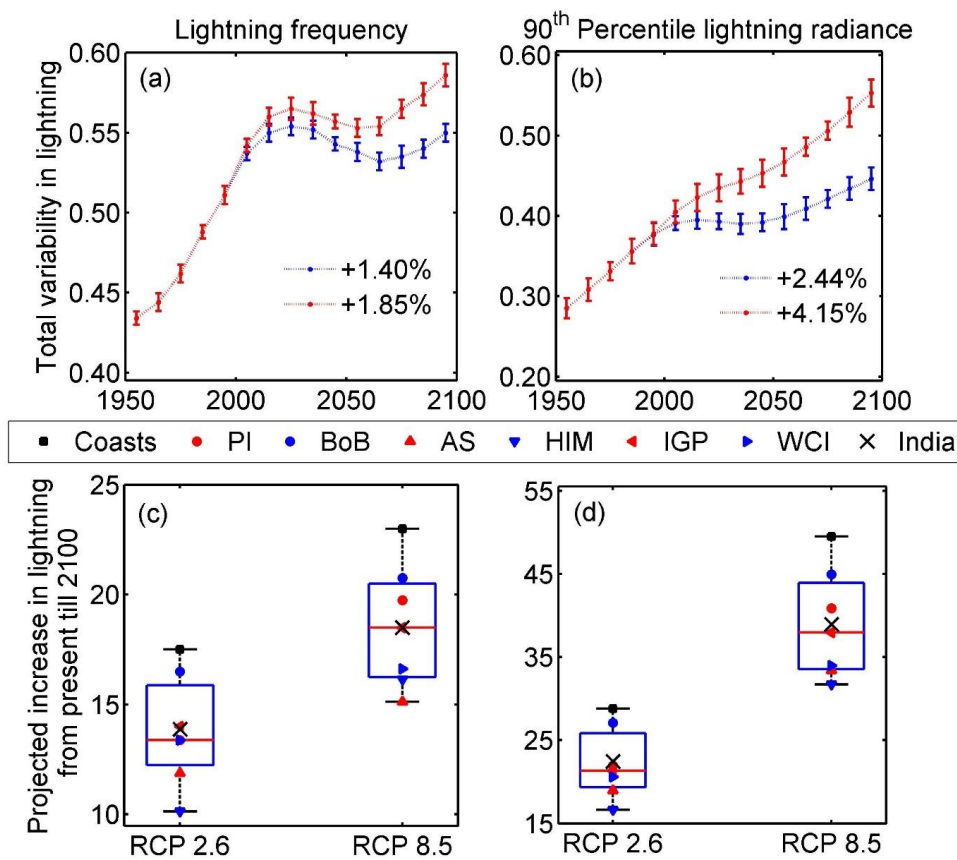
780

781

782



783



784

785 **Figure 7:** 150-year multi-model all-India average projections of (a) lightning occurrences and (b) 90<sup>th</sup> percentile radiance  
 786 using RCP 2.6 and RCP 8.5 scenarios (c,d) Zonal distribution of trends in lightning occurrence and intensity between present  
 787 decade (2011-2020) and 2091-2100

788

789

790

791

792

793

794

795

796

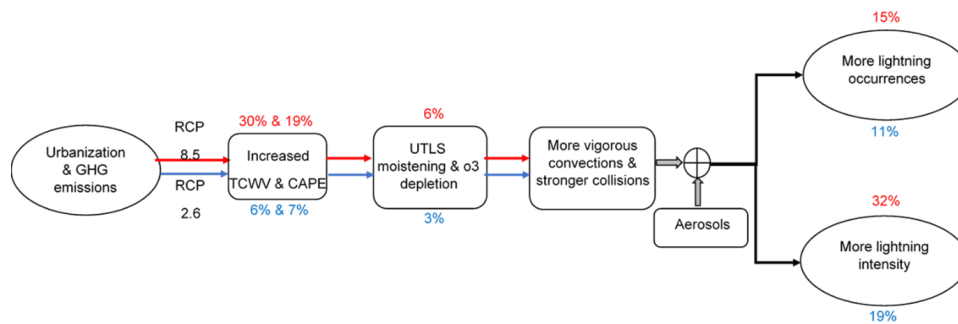
797

798

799



800



801  
802  
803

**Figure 8:** Proposed hypothesis to explain the long-term growth in lightning properties assuming RCP 2.6 and 8.5 over Indian region